Science & Technology Facilities Council

Technical Report
RAL-TR-2016-012

A thermal impulse method to measure the strength of conducting materials at high temperatures and strain rates

JRJ Bennett

September 2016

Enquiries concerning this report should be addressed to:

RAL Library
STFC Rutherford Appleton Laboratory
Harwell Oxford
Didcot
OX11 0QX

Tel: +44(0)1235 445384
Fax: +44(0)1235 446403
email: libraryral@stfc.ac.uk

Science and Technology Facilities Council reports are available online at: http://epubs.stfc.ac.uk

ISSN 1358-6254

UKNF/Target/N10/2016
8 September 2016

A Thermal Impulse Method to Measure the Strength of Conducting Materials at High Temperatures and Strain Rates.

J. R. J. Bennett

Rutherford Appleton Laboratory, Chilton, Didcot, Oxon. OX11 0QX

A Thermal Impulse Method to Measure the Strength of Conducting Materials at High Temperatures and Strain Rates.

Abstract

A method of measuring the strength of conducting materials and Young's modulus of elasticity at high temperatures and strain rates is described. A pulse of electrical current is passed through a thin wire at high temperatures to excite a thermal strain oscillation and corresponding stress. At some combination of temperature and stress the wire will fail. The stress is measured by calculation from the current pulse. Measurements have been made on tungsten at temperatures up to ~3000 K, tantalum up to ~2000 K and molybdenum up to ~2000 K, at strain rates of ~10^3 s^{-1}. The frequency of the oscillations gives Young's modulus of elasticity.

While the method is good for measuring ultimate tensile strengths of materials at high temperatures it is limited in the minimum temperature that can be measured. An example is given for tungsten where the strength is not measurable below a temperature of ~700°C.

1. Introduction

This work was initiated by the study of a solid target [1] for a neutrino factory [2]. A 4 MW proton beam pulse, of a few ns length, at 2-10 GeV energy, would impact on a solid target bar, 1-2 cm diameter and 20 cm long, dissipating ~700 kW in the target. The heat generated in the target would radiate at ~1200°C to water cooled surroundings. The high temperature limits the materials to those with both high strength and melting points such as tungsten and molybdenum. With the small surface area of the target and the limited temperature achievable in the target it is necessary to have ~500 targets circulating through the beam so that a new bar is presented to the beam pulse every 20 ms.

It was originally considered that the target could suffer from thermal shock from a single beam pulse causing mechanical failure. It was decided to measure the lifetime under pulsed conditions at similar temperature, stress and strain rates that would be encountered in the neutrino factory target. The equipment could also be used to measure the ultimate strength as a function of temperature of a few candidate target materials.

Most measurements of the strength of materials under shock at high strain rates are made with Hopkinson bars [3]. This method of impact can produce true mechanical shock, where the stress wave exceeds the speed of sound in the material. However, the method is limited to temperatures below ~1000°C. It should be noted that thermal effects can not normally generate true shock.

It was decided to induce thermal shock in specimens by passing a high current pulse through a thin wire. A spare power supply for the ISIS kicker magnets, giving 1 μs pulses up to ~6 kA at repetition rates up to 50 Hz, was used for these tests.

2. Considerations of the wire dimensions

A current pulse is passed down a thin wire causing thermal stress waves in both radial and longitudinal directions[1]. The stress is caused by the sudden change in temperature of the wire and the resultant thermal expansion. However, the inertia of the wire prevents the wire expanding at the rate of the temperature rise, resulting in stress waves [4-7]. These stress waves travel at the speed of sound, *v*, in the material (The velocity of sound in tantalum is ~3.3x10^3 m s^{-1}.) The time taken for the wave to travel the appropriate dimension, *d* (length or diameter) is given by,

$$\tau_s = \frac{d}{v} \tag{1}$$

When the current pulse length, τ_p, is greater than τ_s, there is no shock,

$$\tau_p > \tau_s \quad \text{No Shock Condition} \tag{2}$$

Conversely, shock waves are produced when,

$$\tau_p < \tau_s \quad \text{Shock Condition} \tag{3}$$

In order to simulate an approximately uniform energy density and temperature in the test wire it is important to dimension the wire accordingly. Because the high frequency current pulse initially starts on the surface of the wire and diffuses radially into the wire in a characteristic time τ_I it is necessary to have a wire diameter that is small enough to achieve this well within the length of the current pulse. The characteristic time is given by (see Appendix 1),

$$\tau_I = \frac{a^2}{\kappa} \tag{4}$$

where *a* is the radius of the wire and

$\kappa = \frac{1}{\mu_0 \sigma}$ where μ_0 is the permittivity of free space and σ is the electrical resistivity.

In the experiments the pulse power supply available for use had an approximately square pulse of 1 μs length ($\tau_s = 1\,\mu s$) and amplitude of up to ~6 kA and a repetition rate of up to ~50 Hz. Figure 1 illustrates the various conditions that must be achieved. The calculations are for tantalum at 300°C. It can be seen that to obtain good penetration of the current into the wire the radius needs to be less than 1 mm. However this makes $\tau_p > \tau_s$ and there is no radial shock. However, the wire is ~10 cm long and this gives rise to strong longitudinal shocks. The lack of full current penetration from the start of the pulse is not a problem since the penetration in the latter part of the pulse is excellent and this is the time of peak temperature and least strength.

Generally the condition for shock and good current penetration can be expressed by,

$$\tau_s \geq \tau_p > \tau_I \tag{5}$$

or, in the case of the 1 μs long current pulse,

$$\tau_s \geq 10^{-6} > \tau_I$$

[1] Rotational and violin modes are not excited.

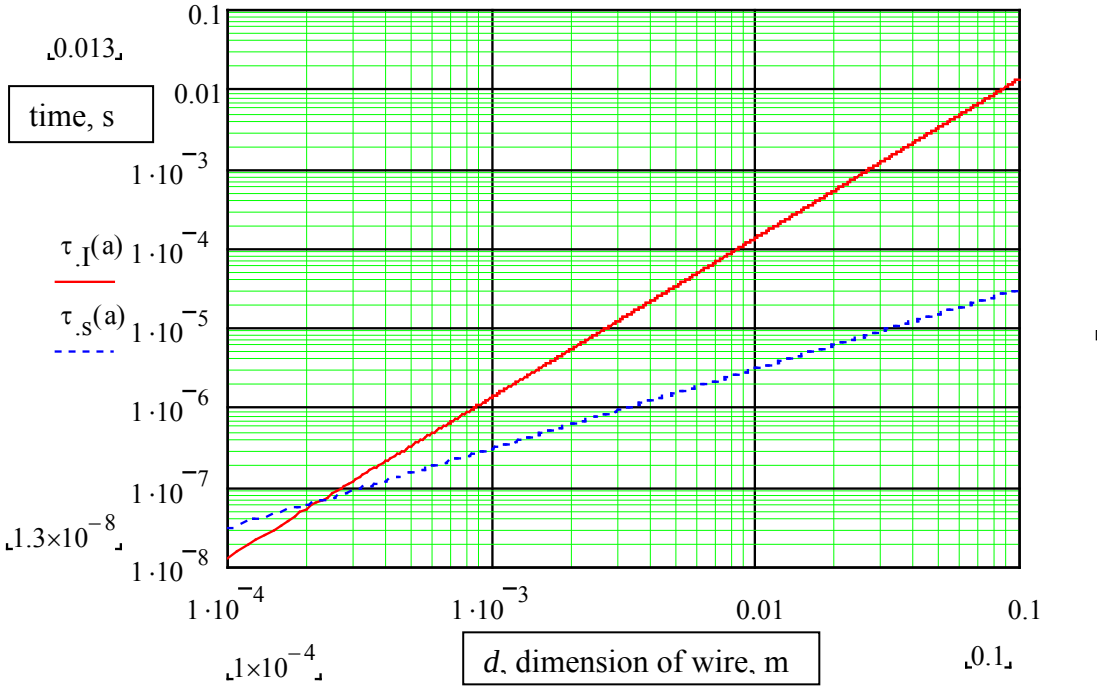

Figure 1. The characteristic time for the radial diffusion of the current into the wire, τ_I, and the value of τ_s as a function of the wire dimensions (radius *a* and length).

A further important consideration is to produce the largest stress in the wire to cover as wide arrange of temperatures as possible. This means the smallest possible wire diameters to produce the maximum energy density from the limited current pulse amplitude. Wires of 0.3 to 1 mm were measured, but most were 0.5 mm diameter. Wires of less than ~0.5 mm diameter were not as reliable as they were found to be too weak to overcome the frictional forces of the graphite jaws in the test equipment. Typically, the wires are 5 to 8 cm long.

Since the longitudinal frequency is several tens of kHz, the periodic time, τ is much longer than the 1 μs current pulse. With a typical wire of ~5 cm length the frequency is ~25 kHz and τ is 0.4 ms. In this time the temperature in the wire has time to become uniform with radius. The characteristic thermal time constant is given by [9],

$$\tau_T = \frac{a^2}{\kappa_T} \tag{6}$$

where κ_T is the thermal diffusivity, given by,

$$\kappa_T = \frac{K}{\rho C} \tag{7}$$

K is the thermal conductivity, ρ the density and *C* the specific heat. The diffusivity of tantalum is 2.6×10^{-5} at 2500 K and this gives a thermal characteristic time constant of 2.4 ms or 6 oscillations of the longitudinal vibration. The combination of good current uniformity and good thermal conductivity means that the wire has good radial temperature uniformity over the first few longitudinal vibrations of the wire.

3. Measurements

The temperature of the wire at the start of the pulse is set by adjusting the repetition rate of the current pulse. The amplitude of the current pulse sets the temperature jump and hence the stress generated in the wire. The current initially starts low and the temperature is increased by adjusting the repetition rate. As the desired temperature is approached the current amplitude is increased (and the repetition rate reduced to keep the temperature at the desired level) until the wire fails. Alternatively the current amplitude is set and the repetition rate increased until the wire breaks.

Figure 2 shows the test wire held firmly in a small chuck at one end and free to expand axially at the other through graphite jaws which lightly press on the wire to hold the wire on axis and conduct the pulse current. The current passes down the central conductor and back down the outer of the coaxial arrangement. Four apertures in the outer conductor allow the wire to be viewed. Figure 3b shows a photograph of the test equipment that is shown in section in Figure 2. Figure 3a shows a photograph of the test equipment in its vacuum chamber; the test wire can be seen through one of the windows.

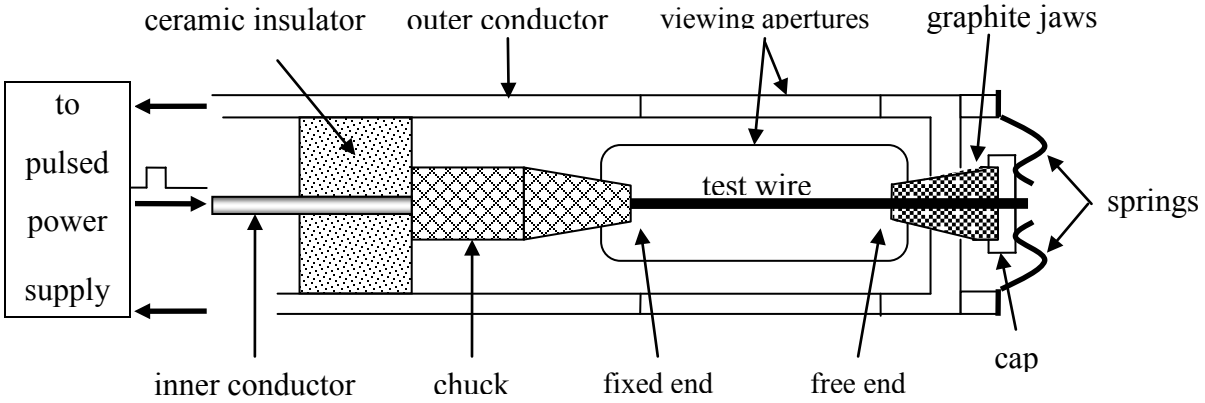

Figure 2. Schematic sectional diagram of the test equipment.

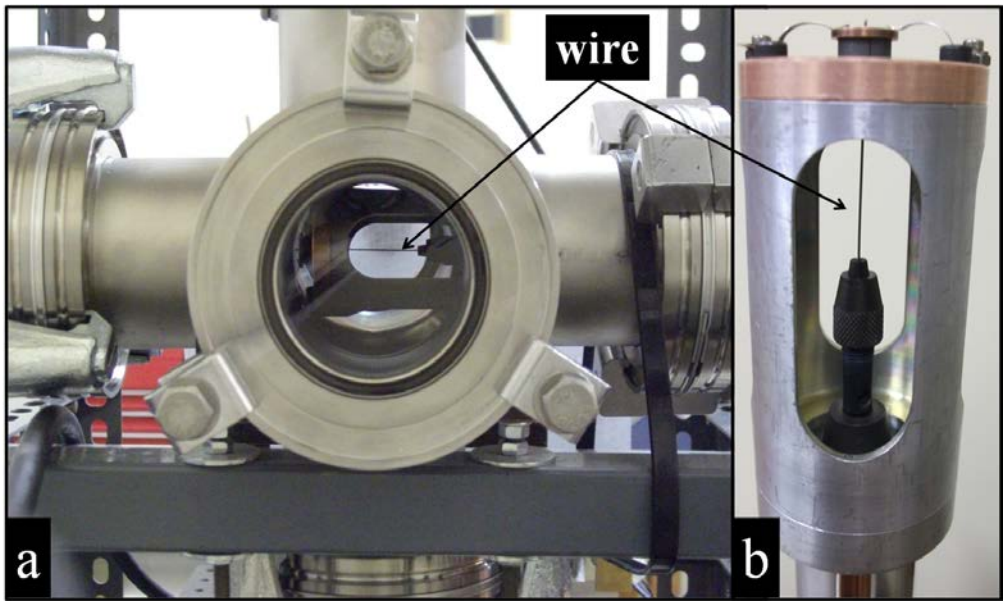

Figure 3a. Photograph of the wire in the vacuum chamber. Fig.3b. Photograph of the wire test assembly.

In operation the wire is hottest approximately at its midpoint. The temperature is nearly constant over a distance of 1-2 cm. Measurements of the radial vibrations and temperature are taken at the hottest point on the wire. The radial and longitudinal variation of temperature is small at this point. Since the temperature along the length of the wire varies greatly, the axial vibrations are not properly defined; in addition there will be some contribution from the whole of the axial conductors supporting the wire.

The oscillations of the wire can be measured by a laser Doppler vibrometer (LDV). The radial frequencies of the oscillations are used to give the value of Young's modulus of elasticity (see Section 5). Figure 4 shows the measured Young's modulus of elasticity [12] versus temperature.

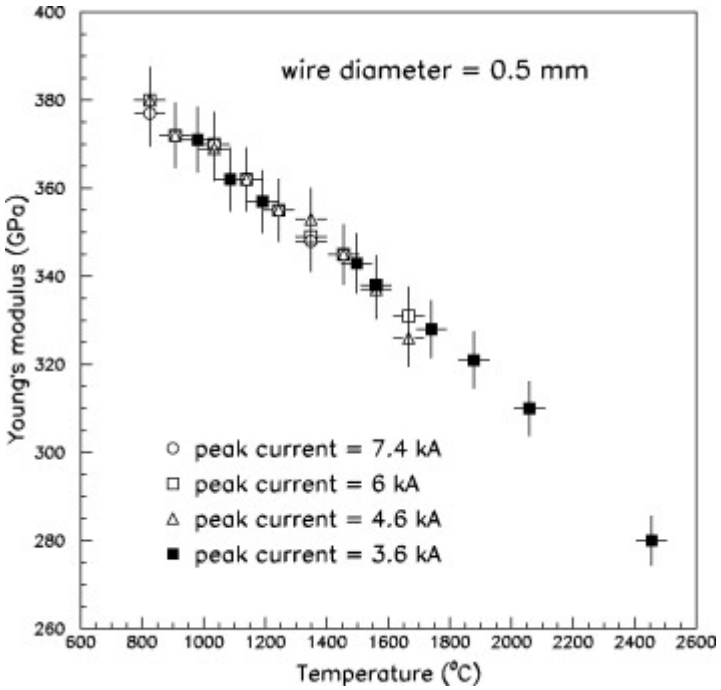

Figure 4. Young's modulus of elasticity of a 0.5 mm diameter tungsten wire as a function of temperature at 4 different peak currents and repetition rates [12].

The yield strength is measured at the temperature and current that the wire starts to show signs of distortion and when the wire physically breaks. Usually the wires of tungsten, tantalum and molybdenum bend before breaking, but occasionally the wires will remain straight but neck down in radius and then break. These are observed by the telescope of a disappearing filament optical pyrometer used to measure the temperature of the wire and also by a screen display from the LDV. The top photograph of Figure 5 [11] shows a hot glowing tungsten wire about to break by bending. The bottom photograph shows a tungsten wire necking down in radius; the pulsed current was turned off at this point to ensure that the photograph could be taken before the wire broke. The bright spot is the laser beam from the LDV.

The radial vibrations of the wire observed by the vibrometer are useful in indicating the onset of failure of the wire. As the wire approaches its yield point the wire becomes plastic and the resonant radial vibrations start to disappear. Figure 6 shows the measured strength of tungsten versus temperature [13] at high strain rates.

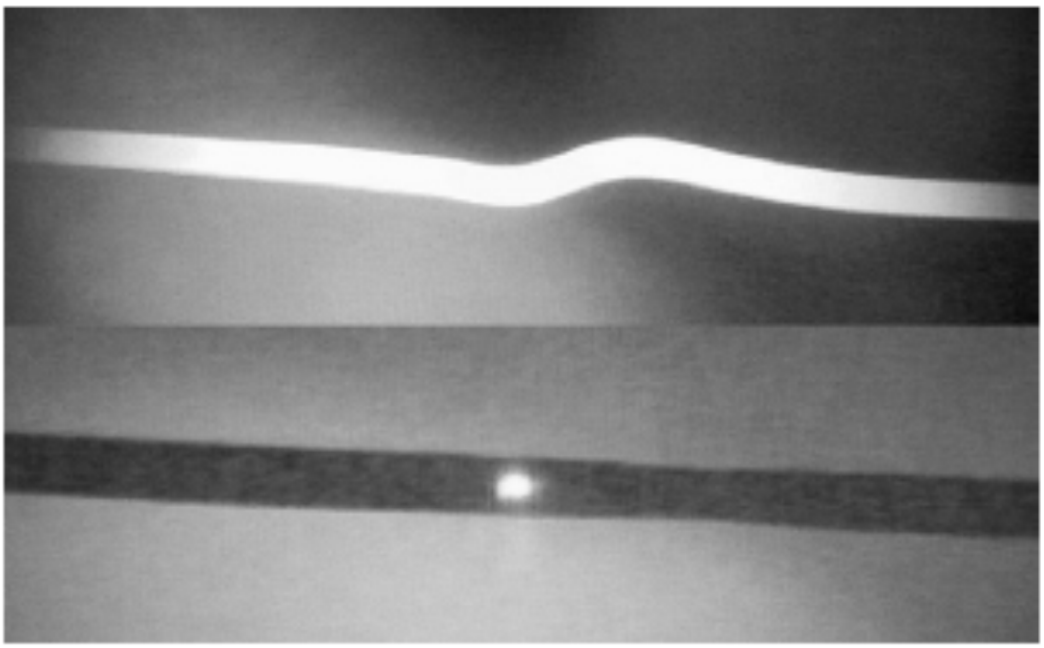

Figure 5. The top photograph shows a hot wire bending before breaking. The bottom photograph is of a wire that has necked down before breaking – wire at room temperature [11].

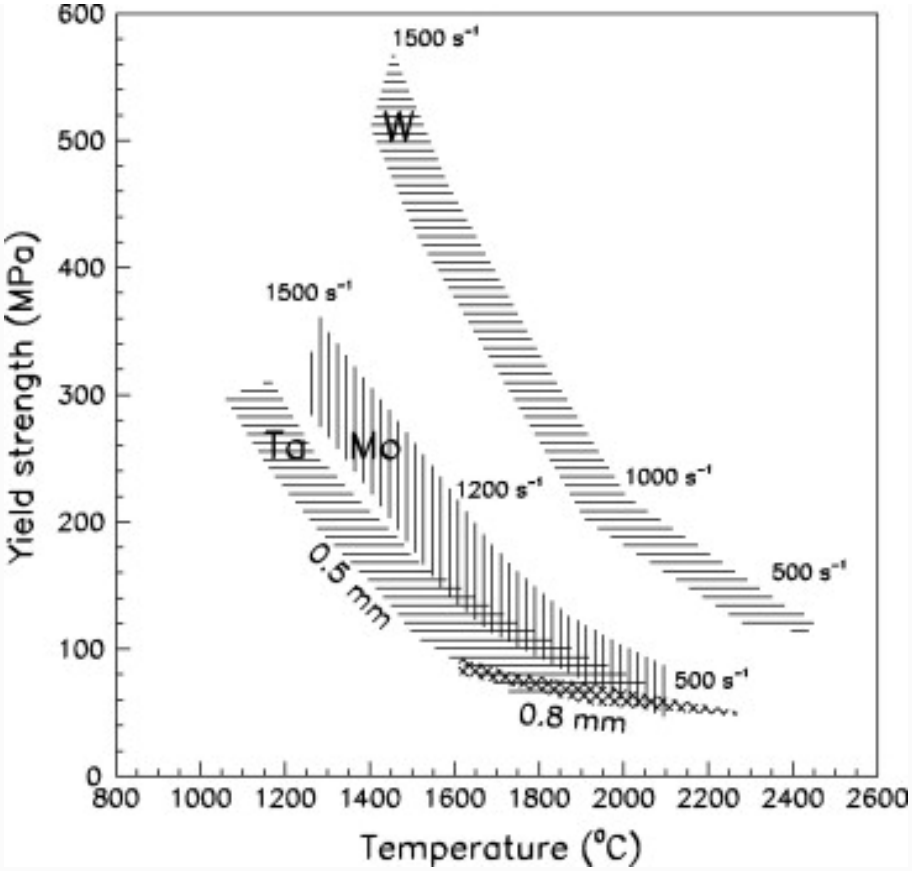

Figure 6. The yield strength versus peak temperature for tantalum wires of 0.5 and 0.8 mm diameter, for tungsten wires of 0.5 mm diameter and for molybdenum wires of 0.5 mm diameter [13]. The upper edge of the bands indicates the stress at which the wire started to bend and the lower edge indicates the stress where the wire was not deformed. The characteristic strain rate values are also shown.

A video of a 0.5 mm diameter iridium wire during testing to breaking point at 2200 K can be accessed by clicking on this link. The wire can be seen to develop wiggles initially and then slip planes. The break in the wire can be seen at the slip plane to the extreme far right of the picture. Iridium has a face centred cubic (fcc) crystal structure whereas tungsten, tantalum and molybdenum have body centred cubic (bcc) crystal structure and do not display slip planes.

The life time of a target under repeated beam current pulses is very important. Tungsten was found to have a good lifetime up to the yield point, see Figure 7 [11]. However, molybdenum, which shows a good high yield stress under conditions of a few pulses, was disappointing in its lifetime, failing typically after ~10000 pulses, even when well under the measured yield stress.

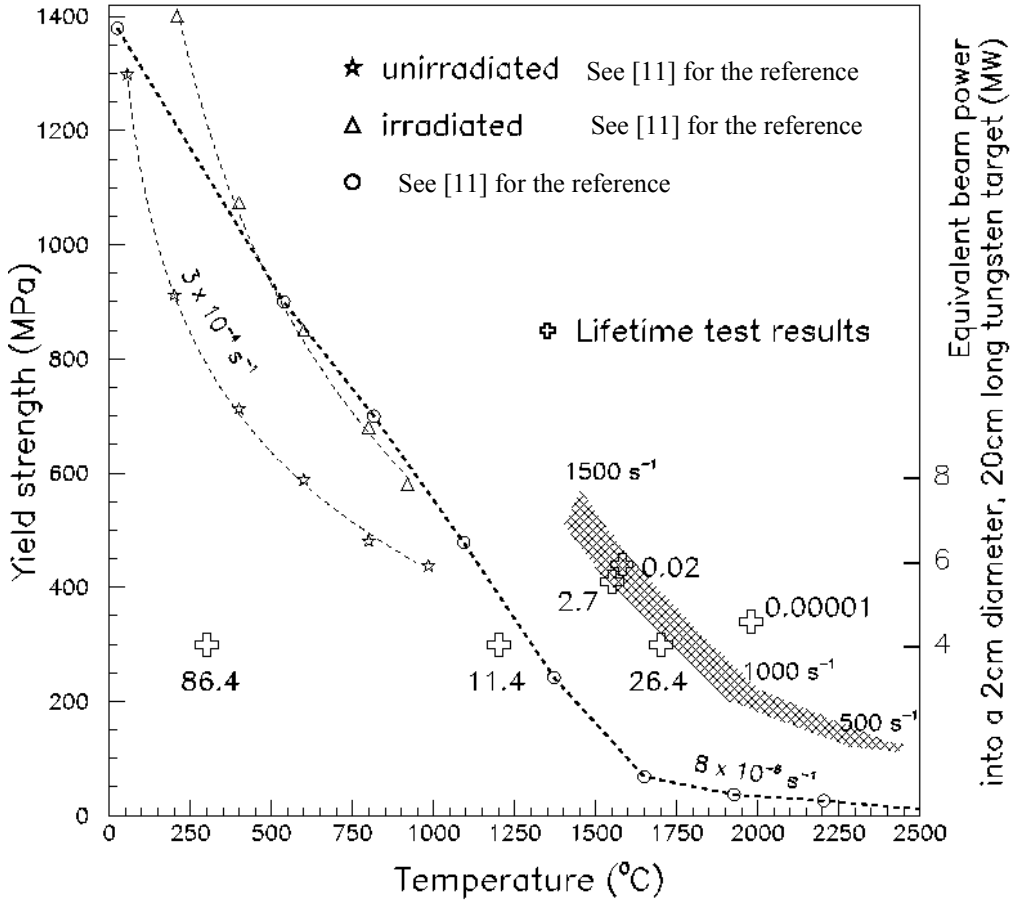

Figure 7. The ultimate yield strength and lifetime of tungsten wires of 0.5 mm diameter versus peak temperature [11]. The upper edge of the band indicates the stress at which the wire deformed or broke after a few pulses and the lower edge indicates where the wire was not deformed. The stress corresponding to the beam power hitting a 2cm diameter target is shown on the right hand side axis. The strain rate is indicated at various points along the curve. The lifetime, in millions of pulses, is shown against the open crosses. Also shown are measured values of yield strength taken at very low strain rates – see [11] for details.

4. The Current Pulse

The current passing through the thin wire is measured by a current transformer. Figure 8 shows the pulse displayed on an oscilloscope. The pulsed power supply consists of a delay line charged to a given voltage and a thyrotron switch. The delay line is not matched to the load, giving rise to a succession of pulses of decreasing amplitude. However, most of the power is in the first pulse and the succeeding pulses can be mainly ignored.

Figure 8. Measured current pulse. Time base 200 ns per cm, y axis 1 kA per cm.

The current pulse has a rise time of ~100 ns, an approximately flat top of ~800 ns and a fall time of ~100 ns. The wire is heated from its initial temperature to a final temperature at the end of the pulse. The heat loss by thermal radiation and conduction is negligible over a few hundred μs. (The radiation cooling of a tungsten wire, of 0.5 mm diameter, by 1 K from 2650 K, takes ~0.1 ms.)

The wire tries to expand during the pulse due to the temperature rise. However, the inertia of the mass of the wire restricts its motion and sets up stress and strain waves in both axial and radial directions. In addition the current in the wire produces a magnetic field which tries to crush the wire radially; this force is released at the end of the pulse.

The current pulse diffuses into the wire from the surface at time $t = 0$. To obtain uniform heating of the wire during the pulse it is necessary to have a small diameter wire. The diffusion equation for the current density as a function of time and radius is given by a solution of Maxwell's wave equation. Assume that an electric field, E, is applied at time t = 0 across the ends of a conductor of circular section, radius, a and length, l. Using Maxwell's equations one arrives at the diffusion equation for the axial current density, j, as a function of time, t, and radius, r, (see Appendix 1 for the derivation)

$$\frac{\partial j}{\partial t} = \frac{1}{\mu_0 \sigma}\left(\frac{\partial^2 j_z}{\partial r^2} + \frac{1}{r}\frac{\partial j_z}{\partial r}\right) \qquad (8)$$

where μ_0 is the permittivity of free space and σ the electrical conductivity. If the electric field or current density,

$$j = \sigma E \qquad (9)$$

is a step then the solution does not fit the measured rise of the current very well. However, if an exponential rise is assumed of the form,

$$j_z = j_{z0}\left(1 - e^{-\gamma t}\right) \tag{10}$$

where the time constant is $1/\gamma$, then the solution to (8) is,

$$j_z = j_{z0}\left[1 - \frac{J_0\left(\sqrt{\gamma r^2/\kappa}\right)}{J_0\left(\sqrt{\gamma a^2/\kappa}\right)}e^{-\gamma t} + \frac{2\gamma}{a\kappa}\sum_{n=1}^{\infty}\frac{e^{-\kappa\alpha_n^2 t}}{\left(\alpha_n^2 - \gamma/\kappa\right)}\frac{J_0(\alpha_n r)}{\alpha_n J_1(\alpha_n a)}\right] \tag{11}$$

where j_{z0} is the current density at $r = a$, α_n are the roots of the Bessel function of the first kind, $J_0(a\alpha) = 0$, $J_1(a\alpha)$ is a Bessel function of the first kind and first order, and $\kappa = 1/\mu_0\sigma$. This can produce an (almost) exact fit to the measured rise time by varying γ; a value of $1/\gamma$ = ~50 ns is a good choice.

Integrating (11) over the radius of the wire gives the current as a function of time. However, the current measured by the current transformer as a function of time gives no information on the current, or current density, as a function of radius. It is not feasible to measure the current density as a function of radius. Hence the assumption that the current density rises exponentially, is a guess, which gives a very good agreement between the measured and calculated current-time profile. Attempts to measure the voltage across the wire were not very effective.

The energy received by the wire during the pulse determines the peak temperature rise. The power density may be integrated over a period of time from 0 to 1 μs (the approximate pulse length) at different radii in the wire. If necessary, the effect of successive pulses due to imperfect matching of the power supply to the load may be evaluated.

In practice, the variation of current with radius in the wire can be ignored. The total power going into the wire can be calculated by integrating the current measured on the current transformer and this is used to give the temperature rise per pulse in the wire.

At the end of the pulse the centre of a tantalum wire has received 87% of the maximum energy density that is delivered to the wire at the outer radius of the wire, $r = a$. Hence, the maximum variation in energy density with radius is only 13%. So the wire receives almost uniform energy density and hence temperature rise and radial thermal stress across the radius. Clearly a smaller diameter wire would perform even better, but wires thinner than ~ 0.5 mm diameter were found to be too weak to overcome the frictional forces of the graphite jaws in the test equipment.

5. Radial and Longitudinal Frequencies

For a bar of length much greater than its radius, the longitudinal frequencies (fundamental, $n = 0$ and harmonics $n = 1,2,3 \ldots$) are given by [4],

$$f_z = \frac{(2n+1)c}{2l} = \frac{2n+1}{2l}\sqrt{\frac{E}{d}} \tag{12}$$

where c is the velocity of sound in the material,

$$c = \sqrt{\frac{E}{d}} \tag{13}$$

E is Young's modulus of elasticity and d is the density of the bar. For a more detailed explanation of the motion of the wire, or bar, see [5,6].

The solution to the radial stress is complicated by the boundary conditions and there is no analytic solution. For a long thin bar, $a << l$, the frequency of oscillation is given by [7],

$$f_n = \frac{\xi_n(\nu)}{2\pi a}\sqrt{\frac{E}{d}\frac{(1-\nu)}{(1+\nu)(1-2\nu)}} \tag{14}$$

where $\xi_n(\nu)$ are the roots of the Bessel equation $\xi J_0(\xi) - \frac{(1-2\nu)}{(1-\nu)} J_1(\xi) = 0$ and ν is Poisson's ratio.

In reality the radial motions couple into the axial and vice versa. These are present in both axes due to Poisson's ratio.

It can be shown that the driving force pulse must be shorter than or not much longer than the period of the oscillation of the longitudinal and radial frequencies. Typically with a tungsten wire of 0.5 mm diameter and ~8 cm length, the radial frequency is ~7 MHz and the longitudinal frequency is ~12 kHz. The thermal pulse generated by the current pulse is ~1 μs long whereas the period of the radial oscillation is ~0.1 μs. Hence the radial oscillation is barely excited by the relatively long current pulse; this is a quasi-static condition. However, the longitudinal oscillation, period ~100 μs, is strongly excited, and strong axial dynamic stresses are produced.

6. The Magnetic Forces

The magnetic pinch force rises up to its plateau level in ~100 ns and remains constant until the end of the current pulse when it decays over ~100 ns. This produces two kicks at the beginning and end of the pulse to produce the radial oscillations. Because the temperature rises during the pulse altering the value of Young's modulus of elasticity, it gives rise to two frequencies corresponding to the start and end of the current pulse. These are observed with the vibrometer to be up to ~40 kHz apart, depending on the pulse current and temperature i.e. the initial and final temperatures. Figure 9 shows the Fourier analysis of the radial velocity signal of a tungsten wire, taken by the vibrometer and displayed on an oscilloscope, during a current pulse. It shows a single pulse (the red line) at a frequency of 6.95 MHz.

Figure 10 shows a similar oscilloscope picture taken at different temperature and pulse current where the double pulse can just be seen. The resolution of the oscilloscope and the natural width of the pulses is assumed to give predominantly single pulses frequently with flattened tops or a peak appearing at the side of the main peak.

The stress is given by,

$$\sigma_m = \frac{\mu_0 I^2}{8\pi^2 a^2} \tag{15}$$

where μ_0 is the permeability of free space. The stress on the surface of a 0.5 mm wire with 6500 A pulse current is 11 MPa.

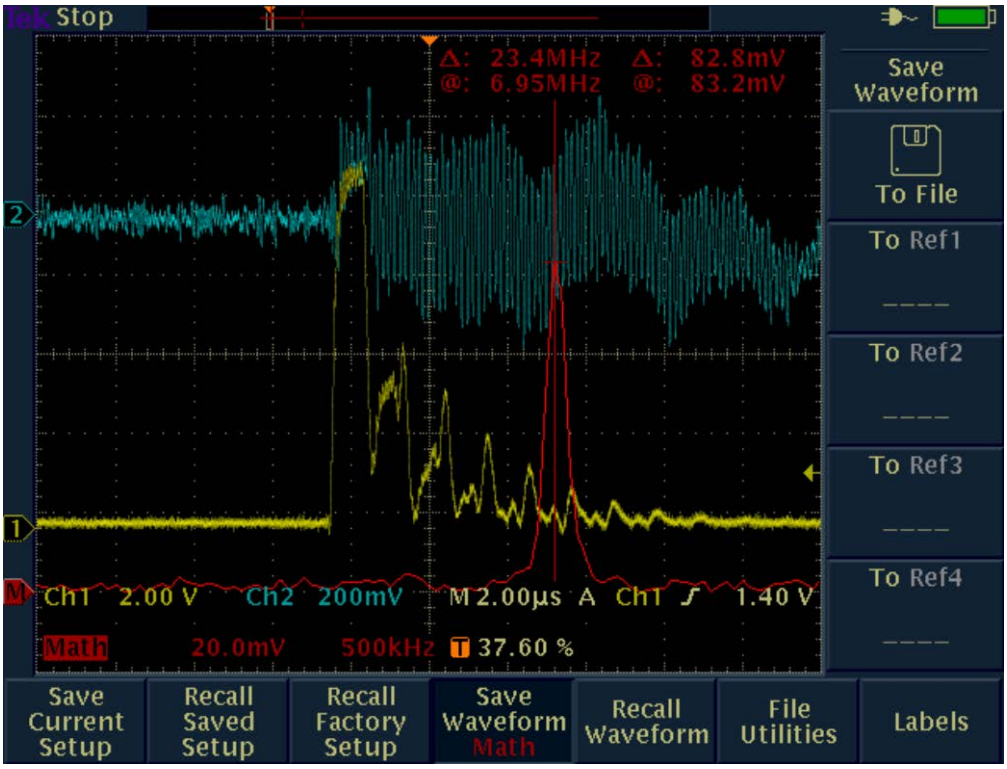

Figure 9. The signals displayed on an oscilloscope of the current pulse (yellow line), the radial velocity (blue line) of a tungsten wire and the Fourier analysis of the radial velocity vibration (red line).

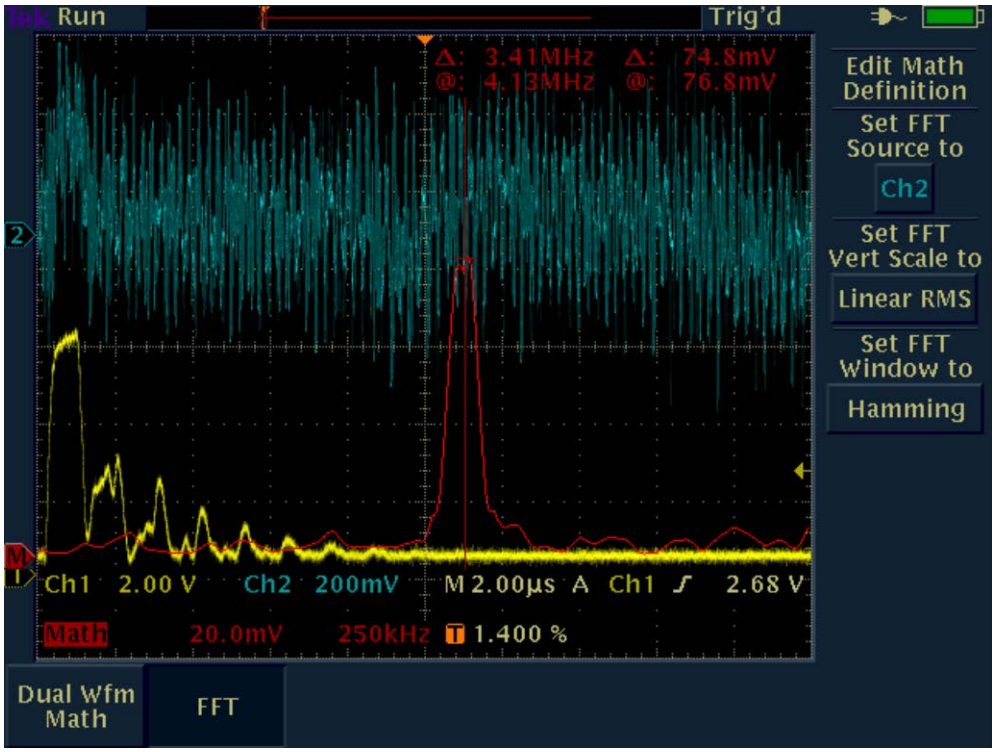

Figure 10. The oscilloscope display as Figure 9, but at a different temperature and pulse current. The double pulse nature of the radial frequency (red line) can be seen.

7. Calculating the Stress in the Wire

The wire suffers an axial thermal stress and a radial magnetic stress due the current pulse in the wire. The solution to the longitudinal stress for a freely suspended bar of length l, Young's modulus of elasticity E, mean coefficient of thermal expansion α and temperature rise ΔT, is [4,8],

$$\sigma(z,t) = \alpha E \Delta T \frac{2}{\pi} \sum_{n=0}^{\infty} \frac{(-1)^n}{(2n+1)} \left[\cos\left(\frac{(2n+1)\pi}{l} (z+ct) \right) + \cos\left(\frac{(2n+1)\pi}{l} (z-ct) \right) \right] \tag{16}$$

where $n = 0,1,2,3,\ldots$ and z is the axial distance from the centre of the bar. This represents two waves travelling in opposite directions and gives a square wave. The amplitude of the stress is,

$$\sigma_0(T) = \alpha(T) E(T) \Delta T \tag{17}$$

Note that the axial stress amplitude is not a function of the length; this stress applies to all axial positions. The peak amplitude stress occurs at the point of greatest temperature rise in a pulse, corresponding to the hottest region of the wire. This is also the weakest part of the wire, since the strength decreases with temperature, and hence the wire always fails at the hottest region. Both α and E are functions of T; since both functions decrease with temperature, the peak pulse temperature should be used when calculating the peak stress.

At 2000 K Young's modulus of elasticity in tungsten is ~325 GPa, the coefficient of thermal expansion is ~6×10^{-6} K^{-1}, the stress for a temperature rise of 160 K with 6500 A pulse current is ~330 MPa. This stress is thirty times larger than the magnetic stress generated by the current pulse. Since both the temperature rise and the magnetic stress are proportional to the square of the current, the thermal stress will always be much larger than the magnetic.

As a result, the stress in the wire is, to a good approximation, simply the axial thermal term given by (17). Measurement of the temperature jump, ΔT, from a pulse of current and a knowledge of the thermal expansion, α, gives the stress.

The temperature jump may also be expressed in terms of the current I, the resistivity of the wire ρ, the radius of the wire a, the density of the material of the wire d, the specific heat S and the duration of the pulse τ.

$$\Delta T = \frac{I^2 \rho \tau}{\pi^2 a^4 S d} \tag{18}$$

which then gives the stress as,

$$\sigma_0 = \frac{\alpha E I^2 \tau \rho}{\pi^2 a^4 S d} \tag{19}$$

Almost all the parameters in (19) vary with temperature.

Equation (18) may be expressed for a small change in temperature in a short time dt in terms of the parameters which change with temperature as,

$$dT = \frac{I^2 \rho(T) dt}{\pi^2 a(T)^4 S(T) d(T)} \tag{20}$$

All the parameters which change with temperature can be expressed in terms of polynomials of temperature [10]. Integration of (20) gives,

$$\int_{T_1}^{T_2} \frac{a(T)^4 S(T) d(T) dT}{\rho(T)} = \frac{I^2}{\pi^2} \int_0^{\tau} dt \tag{21}$$

where T_2 is the peak temperature at the end of the current pulse and T_1 is the temperature at the beginning of the pulse.

When the delay line of the power supply is well matched to the load there is a single square pulse and the right hand side of (21) is simply $\frac{I^2\tau}{\pi^2}$. If the delay line and load are not matched there can be a series of pulses of diminishing amplitudes reflected between the load and delay line. In this case the current, which is recorded on an oscilloscope and saved to a computer, can be integrated over time to give the total charge passing through the wire. In the case of good matching, (21) can be expressed as,

$$\int_{T_1}^{T_2} \frac{a(T)^4 S(T) d(T) dT}{\rho(T)} - \frac{I^2}{\pi^2}\tau = 0 \qquad (22)$$

From equation (21) or (22) the value of T_1 can be calculated for the measured value of the peak pulse temperature, T_2, and hence the temperature rise in a single pulse is obtained, $\Delta T = T_2 - T_1$. (Or, if the temperature, T_1, is measured just before the pulse, then T_2 can be calculated. Alternatively, both T_1 and T_2 can be measured to give directly ΔT.) Then the stress may be calculated from (17) with the appropriate values of α and E at the peak pulse temperature, T_2.

Figure 11 shows the values of ΔT as a function of T_2 for different pulse currents; A linear relation fits the calculated data to high accuracy (the quality of the fit is given by $R^2 = 1$, from Excel) and the equations are shown for each of the currents plotted. These equations scale approximately as the square of the current, as would be expected from (18), where the variation of the parameters in (18) are ignored.

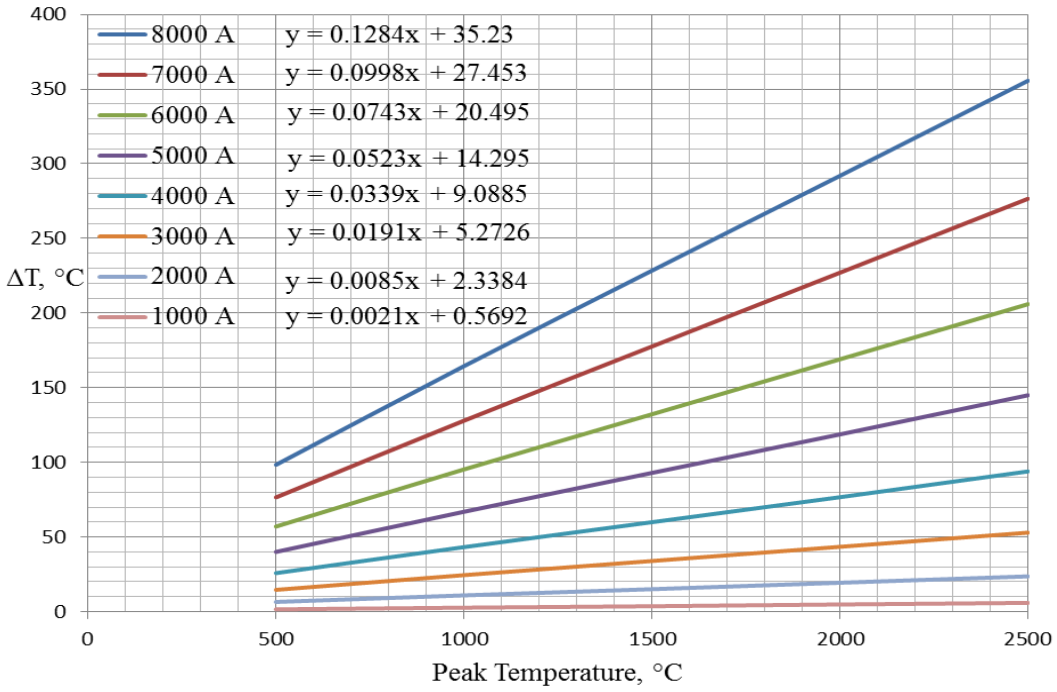

Figure 11. The pulse temperature rise in a tungsten wire as a function of peak temperature for constant pulse current. The equations for the fitted lines have axes y corresponding to ΔT and x to T_2.

The same data is shown in Figure 12, with ΔT plotted against pulse current I for constant values of peak temperature T_2. In this case a polynomial is fitted to the curves (y corresponds to ΔT and x to the pulse current, I, $R^2 = 1$ in all cases).

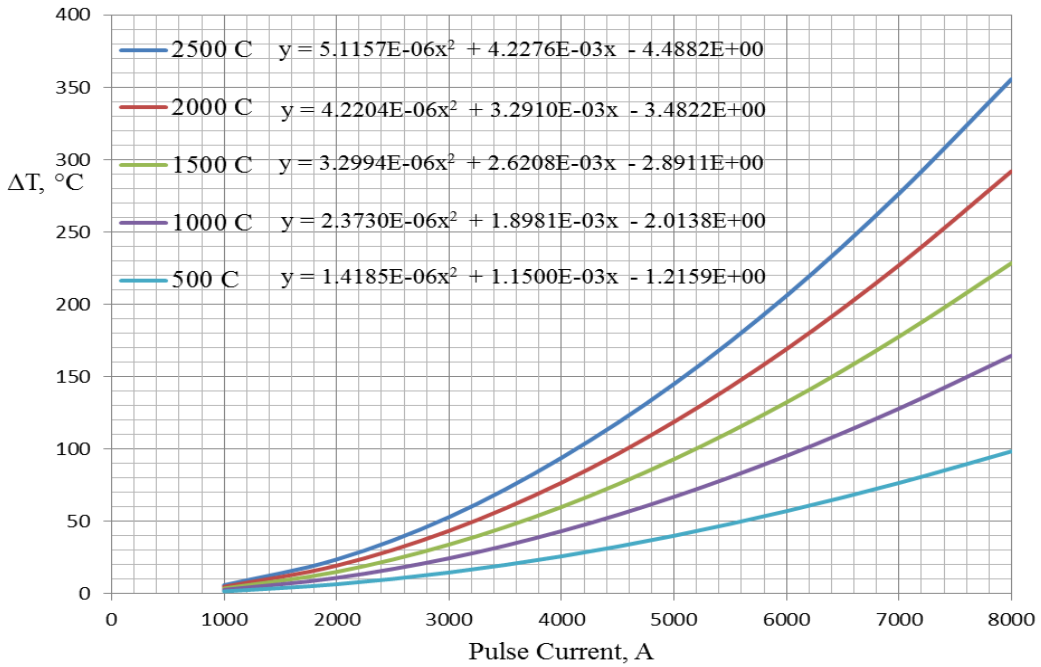

Figure 12. The pulse temperature rise, ΔT, as a function of pulse current, I, for constant peak temperatures, T_2. Tungsten wire.

Using equation (17) the ultimate tensile strength of the wire can be found. Figure 13 shows the results for pulse currents of 8000 and 6000 A.

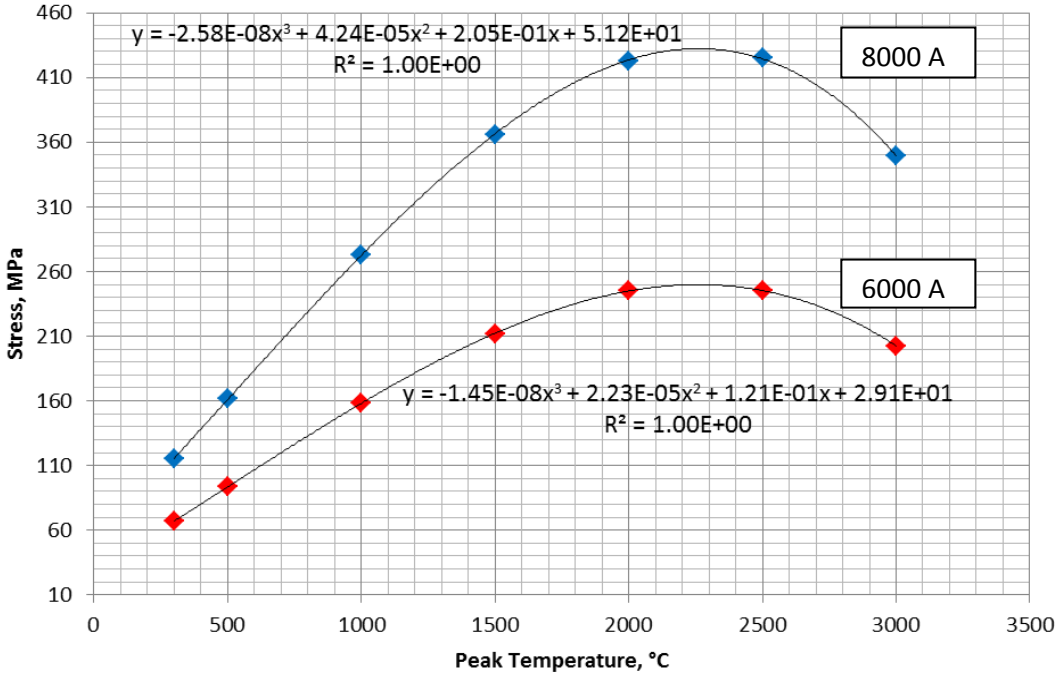

Figure 13. Stress in the tungsten wire for pulse currents of 8000 A and 6000 A versus the peak temperature of the wire. A third order polynomial has been fitted to the points and is shown by the solid black lines.

8. Finite Element Analysis

It was initially thought that there might be real shock (a stress wave exceeding the velocity of sound in the material) generated in the target by the thermal shock. Therefore, a finite element dynamic code, LS-DYNA, was used to calculate the stress in the wire from the current. It was not until some time later that the authors realised that this was not possible. The diffusion of the current was calculated from the analytical relation of the diffusion of the current into the wire (see Section 4 and Appendix 1). A non-dynamic code was used later, which confirmed that the results were identical to those using the dynamic code. Detailed calculations of the radial oscillations of the wire were made and compared with the measurements taken from the Vibrometer. Agreement was strikingly good [11]; see Figures 14 and 15 for a comparison of the calculated and measured radial velocities and longitudinal velocities of a 0.5 mm diameter tungsten wire. The details of the diffusion of the current and the wire temperature versus radius, length and time are necessary for the calculations of these motions.

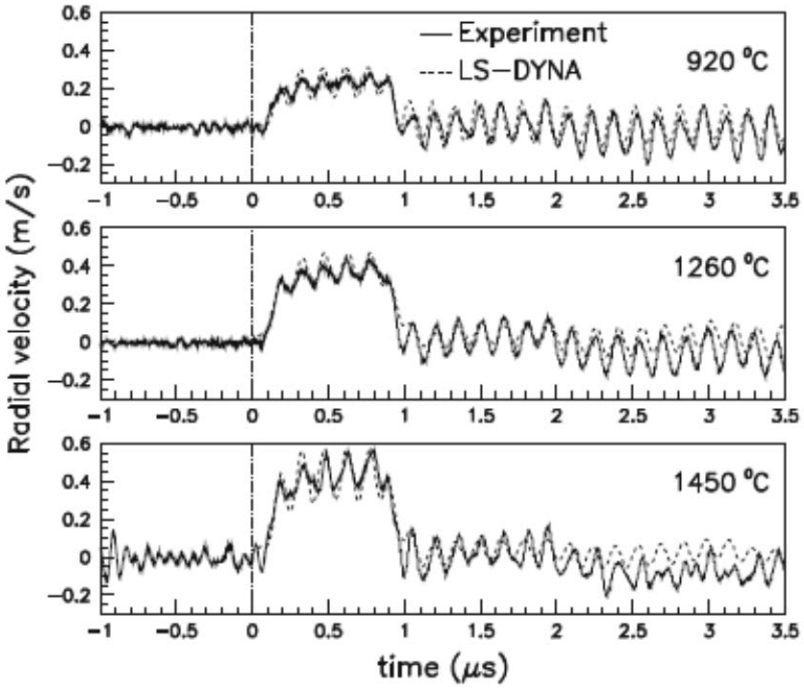

Figure 14. Measured and calculated radial velocity of a 0.5 mm diameter tungsten wire at peak temperatures of 920, 1260 and 1450°C [11].

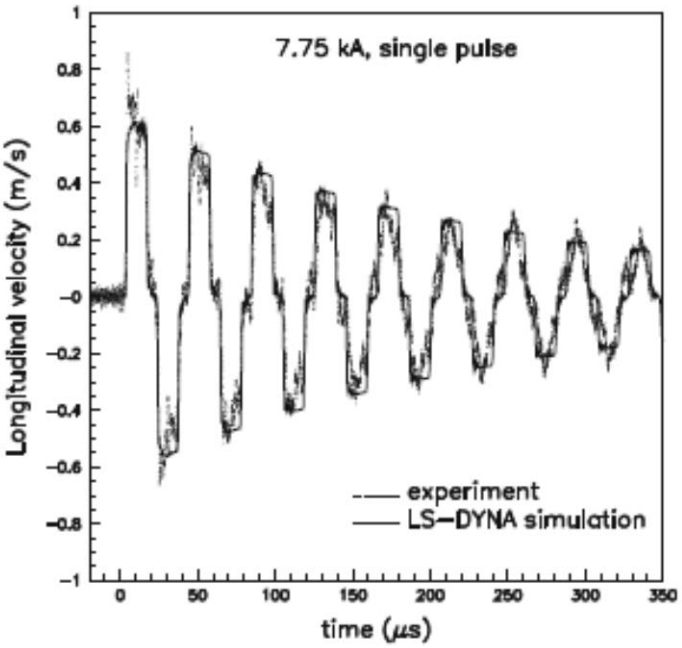

Figure 15. Measured and calculated longitudinal velocity (dotted line) of the end of a 0.5 mm diameter tungsten wire [11]. Single pulse mode, current pulse 7.75 kA and the wire close to room temperature.

The results from tests to measure the strength and Young's modulus of elasticity on tungsten, tantalum and molybdenum have already been published [11-14] – and see Section 3. Comparisons of the analytic and finite element results for the strength show no appreciable difference within the experimental error of the measurements. Since the analytic method is much quicker to perform, future measurements will be treated in this way.

9. Measurements of Strength at Lower Temperatures

The measurements are limited to minimum temperatures of ~1200°C by the maximum current from the power supply. Skoro [14] has fitted a curve to the strength data for tungsten using a formula for shock in materials by Zirilli and Armstrong [15]; Figure 16 shows the result (the green curve) which has been extended to a low temperature of 0°C. The formula may not be very accurate for such a large extrapolation and it really applies to true shock rather than thermal shock. In addition, tungsten suffers from a brittle to ductile transition between ~200°C - 400°C; so the strength versus temperature curve may suffer a discontinuity.

For comparison with the high strain rate measurements, the ultimate tensile strength of tungsten at ~zero strain rates is also shown in Figure 16. There is considerable data on tungsten in both annealed (recrystallized) and stress relieved (cold worked) conditions. The lines are an "average" of the measurements given in [10].

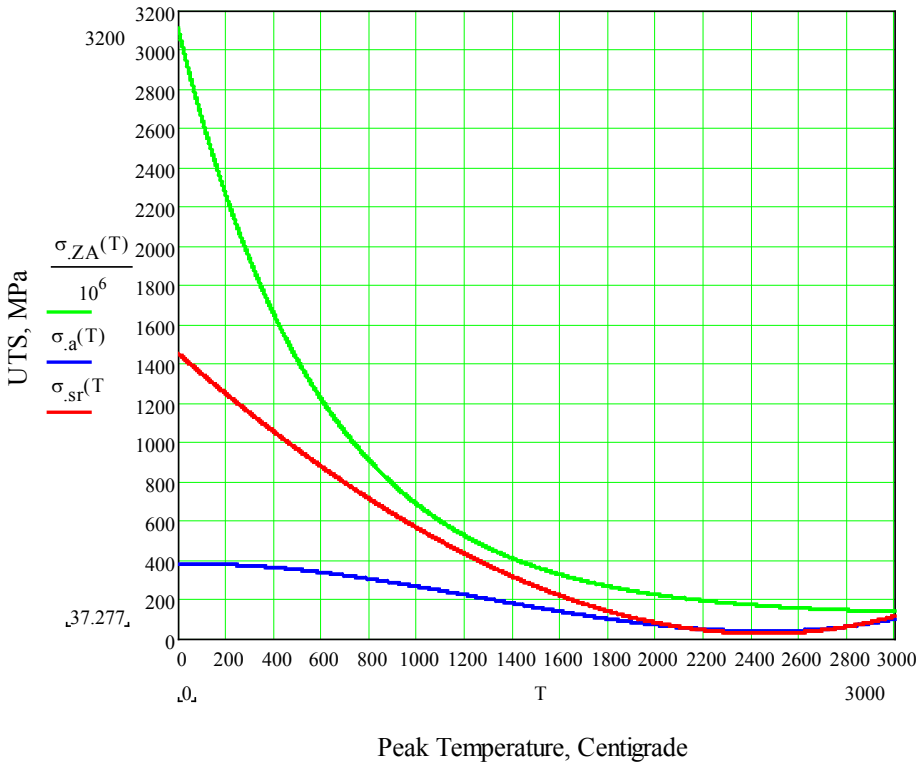

Figure 16. The ultimate tensile strength of tungsten versus temperature. Green line, the Zirilli Armstrong prediction [14,15], strain rate 10^3 s^{-1}. Blue line, annealed tungsten, measurements at low strain rate. Red line, stress relieved tungsten, measurements at low strain rate.

To extend the measurements to lower temperatures a power supply capable of delivering current pulses of ~30 kA is being built. Using equation (17) and equating the stress to the breaking stress calculated by Skoro [14], gives the peak temperature rise, ΔT, required to break the 0.5 mm diameter tungsten wire as a function of the peak temperature, T, at the end of the current pulse. Figure 17 shows the value of the temperature rise, ΔT. Also shown is the temperature required at the start of the pulse, the blue curve, and the red curve gives the final temperature, T (this is the same as the x axis value). Note that T is the T_2 of equation (21) and the blue curve is T_1.

Figure 17 is quite revealing; since it is impracticable to have the wire much below ~0°C at the start of the pulse, then the peak temperature cannot be below ~650°C and ΔT cannot exceed 650°C. In other words, it is not possible to measure the strength of tungsten below 650°C with this method. A current of 24.6 kA is required for this temperature rise in tungsten.

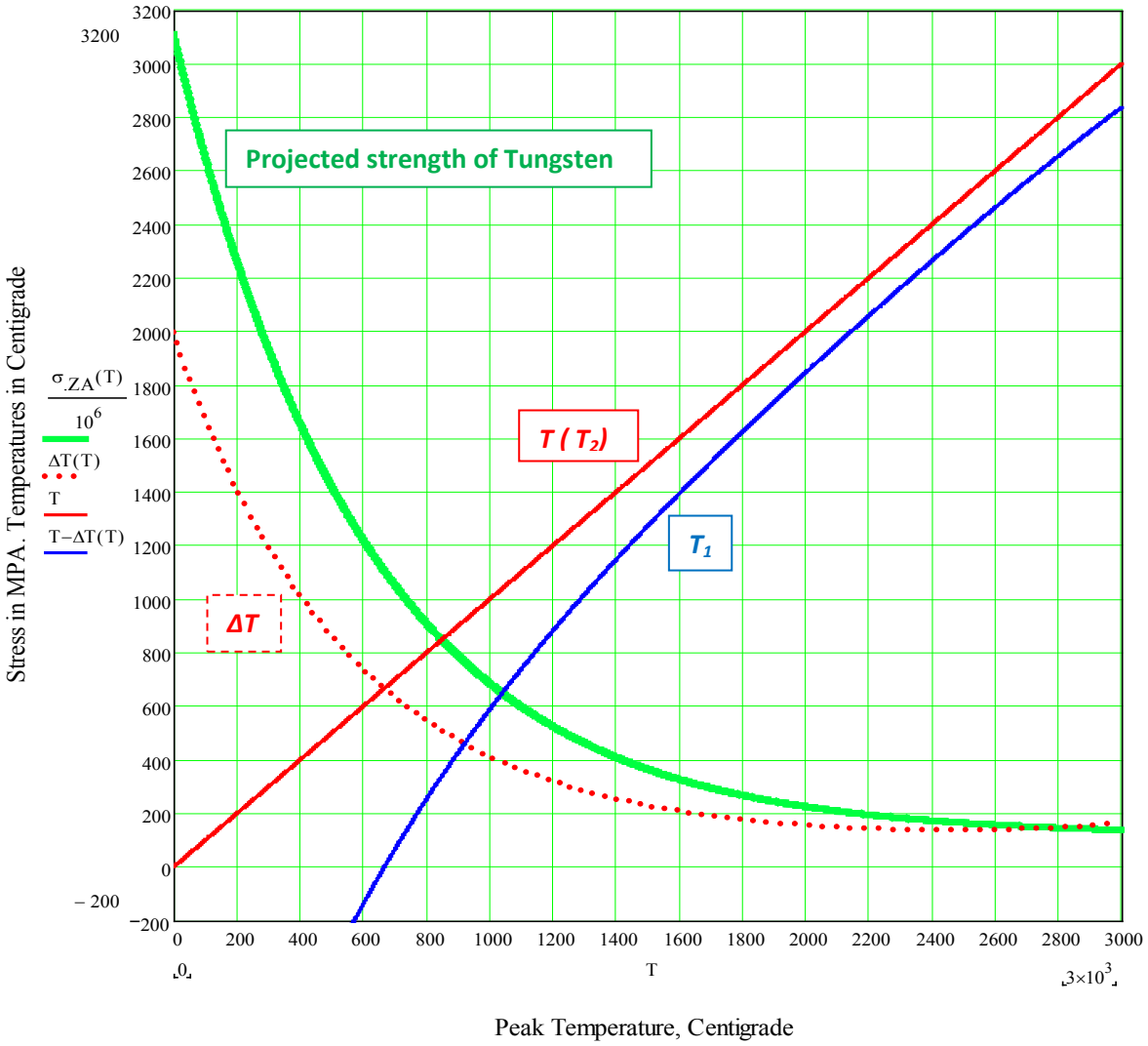

Figure 17. The green curve shows the strength of tungsten versus temperature, °C, taken from Skoro [14] and extended to 0°C. The dotted red curve shows the ΔT required in a single pulse to break the wire. The solid red curve is the final temperature (T_2) during the pulse and the blue curve is the temperature of the wire at the beginning of the pulse (T_1).

Acknowledgements

The author would like to acknowledge the work of Goran Skoro in taking the measurements and calculating the results. It was a pleasure to work with him. Also, I would like to acknowledge the help of Claire Baker when measuring iridium wires and in particular taking the video on her mobile phone of a wire breaking.

Many thanks to Adrian McFarland, Kenny Rodgers and the members the team who generously supported the use of the ISIS kicker magnet power supplies. Without them the work would never have succeeded. Finally, I would like to thank Rob Edgecock for his unfailing support and the provision of the various grants which funded this work.

References

[1] J. R. J. Bennett et al. Journal of Nuclear Materials 377(1) (2008) 285-289.

[2] See the proceedings of NuFactfrom 1999 onwards, e.g. NuFact 2005; Nucl. Phys. B 155 (2006) (Proc. Suppl.)

[3] J. E. Field, S. M. Walley, W. G. Proud, H. T. Goldrein, C. R. Siviour, Int. J. Impact Eng., 30 (2004) 725.

[4] A. E. H. Love, A Treatise on the Mathematical Theory of Elasticity, Cambridge University Press, 2nd Edition 1906.

[5] JRJ Bennett (STFC Rutherford Appleton Lab.), Understanding the Motion of a Long Bar under Electric Pulse Heating; Stress, Strain and Strain Rate.
RAL Technical Reports RAL-TR- 2016-009. 2016.

[6] JRJ Bennett (STFC Rutherford Appleton Lab.), Free Vibrations of a Solid Cylinder,
RAL Technical Reports RAL-TR- 2016-010. 2016.

[7] J. R. Airey, Archiv der Mathematik und Physik. Series 3, Volume 20 (1913) 289.

[8] P. Sievers, CERN Report, LAB. II/BT/74-2, 1974.

[9] H. S. Carslaw and J. C. Jaeger, Conduction of Heat in Solids, Oxford University Press, 1959.

[10] J. W. Davis et al, ITER Materials Property Handbook, 1997, Volume AM01-2111.

[11] J.R.J. Bennett, G.P. Skoro et al, Nuclear Instruments and Methods in Physics Research A, 646 (2011) 1-6.

[12] Skoro, J.R.J. Bennett et al, Journal of Nuclear Materials 409 (2011) 40-46.

[13] G.P. Skoro, J.R.J. Bennett et al, Journal of Nuclear Materials 426 (2012) 45-51. G.P.

[14] G. P. Skoro, J.R.J. Bennett et al, arXiv:1105.5514v1 [cond-mat-mtrl-sci] May 2011

[15] F. J. Zirilli and R. W. Armstrong, Journal of Applied Physics 61 (1987) 1816-1825.

Appendix 1. The Current Density in the Wire under Transient Conditions

Assume that a current pulse I is applied to the long conductor of radius a at time $t = 0$. In practice a current can not be instantaneously applied but a voltage or electric field can. Thus, assume that an electric field E is instantaneously applied across the conductor. The current density j flowing through the conductor is assumed to be circularly symmetric about the axis of the conductor. Using Maxwell's equations and assuming that the electric and magnetic fields, H, are instantaneously propagated so that the displacement current is neglected[2],

$$\text{curl}\underline{H} = \underline{j} \qquad \text{A1(1)}$$

$$\text{curl}\underline{E} = -\frac{\partial \underline{B}}{\partial t} \qquad \text{A1(2)}$$

where B is the magnetic induction.

$$\sigma\underline{E} = \underline{j} \qquad \text{A1(3)}$$

$$\underline{B} = \mu_0 \underline{H} \qquad \text{A1(4)}$$

which gives

$$\text{curl}\underline{B} = \mu_0 \underline{j} \qquad \text{A1(5)}$$

and

$$\rho\text{curl}\,\underline{j} = -\frac{\partial \underline{B}}{\partial t} \qquad \text{A1(6)}$$

Taking the time derivative of A1(5)

$$\frac{\partial(\text{curl}\underline{B})}{\partial t} = \mu_0 \frac{\partial \underline{j}}{\partial t} \qquad \text{A1(7)}$$

and substituting for B from A1(6)

$$\frac{1}{\mu_0\sigma}\text{curl}\left(\text{curl}\,\underline{j}\right) = -\frac{\partial \underline{j}}{\partial t} \qquad \text{A1(8)}$$

This can be re-expressed by using the relation,

$$\text{curl}\left(\text{curl}\,\underline{j}\right) = \text{grad}\left(\text{div}\,\underline{j}\right) - \text{div}\left(\text{grad}\,\underline{j}\right) \qquad \text{A1(9)}$$

so A1(8) becomes,

$$\frac{\partial \underline{j}}{\partial t} = -\frac{1}{\mu_0\sigma}\left[\text{grad}\left(\text{div}\,\underline{j}\right) - \text{div}\left(\text{grad}\,\underline{j}\right)\right] = \frac{1}{\mu_0\sigma}\text{div}\left(\text{grad}\,\underline{j}\right) \qquad \text{A1(10)}$$

since the only component of j is axial, resulting in

$$\text{div}\,\underline{j} = \frac{\partial j_z}{\partial z} = 0 \qquad \text{and hence} \qquad \text{grad}(\text{div}\,\underline{j}) = 0 \qquad \text{A1(11)}$$

Expressing A1(10) in cylindrical co-ordinates,

$$\frac{\partial \underline{j}}{\partial t} = \frac{1}{\mu_0\sigma}\left(\frac{\partial^2 j_z}{\partial r^2} + \frac{1}{r}\frac{\partial j_z}{\partial r}\right) \qquad \text{A1(12)}$$

[2] The error is negligible when the wavelengths are large compared to the dimensions of the system. See:- Static and Dynamic Electricity, W. R. Smythe, McGraw-Hill Book Co. Inc. New York, 1968.

This is the diffusion equation[3] and can be solved for the case of a current density, j_{z0}, (or electric field, E) applied instantaneously at time $t = 0$ and initially $j_z = 0$ within the conductor. For $t > 0$,

$$j_z = j_{z0}\left[1 - \frac{2}{a}\sum_{n=1}^{\infty} e^{-\kappa\alpha_n^2 t}\,\frac{J_0(r\alpha_n)}{\alpha_n J_1(a\alpha_n)}\right] \qquad \text{A1(13)}$$

where j_{z0} is the current density at $r = a$, α_n are the roots of the Bessel function of the first kind, $J_0(a\alpha) = 0$, $J_1(a\alpha)$ is a Bessel function of the first kind and first order, and $\kappa = 1/\mu_0\sigma$. Figure A1-1 shows the variation of j_z/j_{z0} with r/a for certain values of $\kappa t/a^2$.

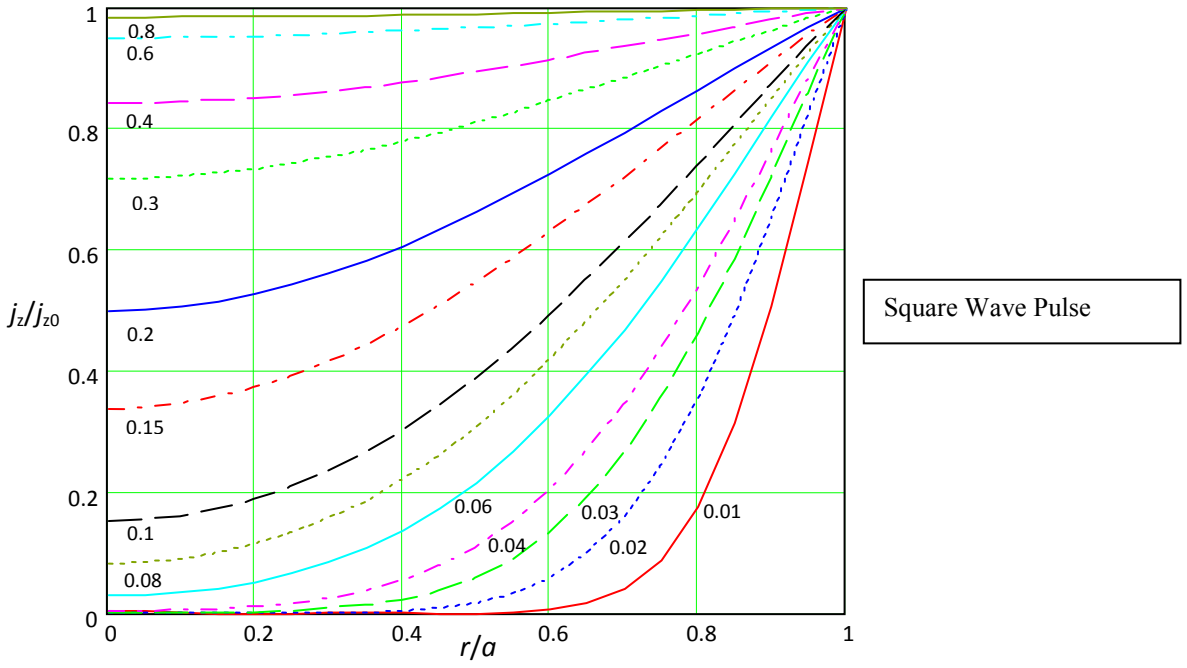

Figure A1-1. Variation of the relative current density with r/a at different values of $\kappa t/a^2$.

Note that the application of a steady state sinusoidal current gives an alternative solution to Maxwell's equations and gives rise to the concept of skin depth.

Figure A1-2 shows the same curves, but the dimensionless $\kappa t/a^2$ has been replaced by the time, t, with value of κ chosen for the tantalum wire at 2000 K and the wire radius of 0.2 mm. It should be noted that the remainder of the graphs are expressed in this way and that if a or κ are changed it will change the time marked against the curve. In the case chosen, the current density at the centre of the wire has reached 90% of its maximum value after 300 ns.

[3] Conduction of Heat in Solids, H. S. Carslaw and J. C. Jaeger, Oxford University Press, 1959.

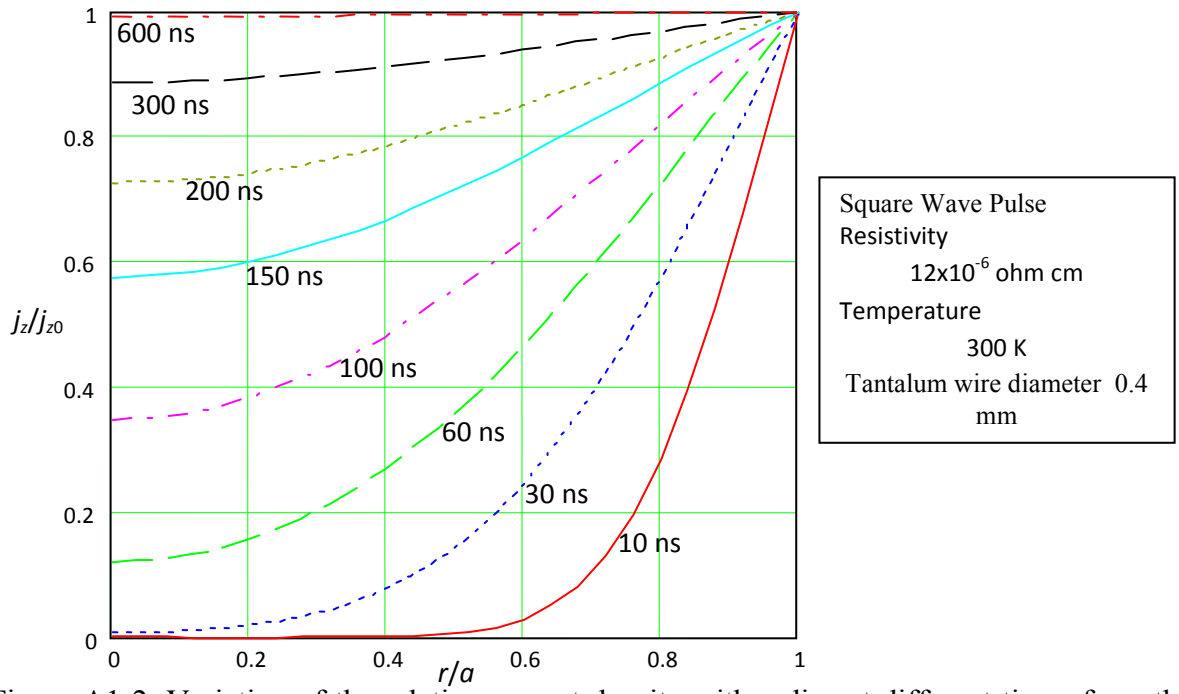

Figure A1-2. Variation of the relative current density with radius at different times from the start of the current pulse.

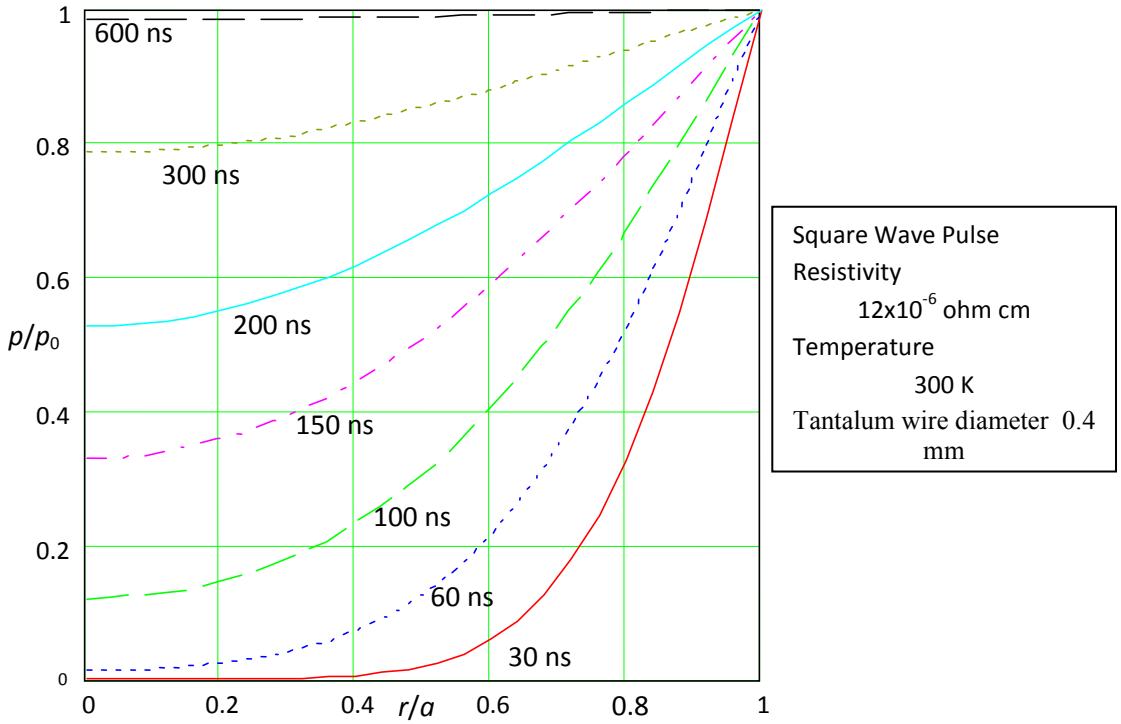

Figure A1-3. Relative power density versus radius at different times.

The power density in the conductor is,

$$p = \frac{j_z^2}{\sigma} \qquad \text{A1(14)}$$

and is shown in Figure A1-3, expressed in terms of the power density, p_0, with $j_z = j_{z0}$. The power density at the centre of the conductor reaches nearly 80% of its full value in 300 ns.

The Solution for an Exponential Rise in Current Density

Assume that the current density in the wire is initially zero and rises with time exponentially at $r = a$ as,

$$j_z = j_{z0}\left(1 - e^{-\beta t}\right) \qquad \text{A1(15)}$$

then [4],

$$j_z = j_{z0}\left[1 - \frac{J_0\left(\sqrt{\beta r^2/\kappa}\right)}{J_1\left(\sqrt{\beta a^2/\kappa}\right)}e^{-\beta t} + \frac{2\beta}{a\kappa}\sum_{n=1}^{\infty}\frac{e^{-\kappa\alpha_n^2 t}}{\left(\alpha_n^2 - \beta/\kappa\right)}\frac{J_0(\alpha_n r)}{\alpha_n J_1(\alpha_n a)}\right] \qquad \text{A1(16)}$$

The current, averaged over the cross-sectional area of the wire is, in terms of the final current, I_0, given by,[4]

$$\frac{I}{I_0} = 1 - \frac{2J_1\left(\sqrt{\beta a^2/\kappa}\right)e^{-\beta t}}{\sqrt{\beta a^2/\kappa}\,J_0\left(\sqrt{\beta a^2/\kappa}\right)} + \frac{4}{a^2}\sum_{n=1}^{\infty}\frac{e^{-\kappa\alpha_n^2 t}}{\alpha_n^2\left[\alpha_n^2\kappa/\beta - 1\right]} \qquad \text{A1(17)}$$

Figure A1-4 shows the result for tantalum wire at 1000°C with $1/\gamma$ = 50 ns and a = 0.25 mm. Comparison (not shown) of the calculated current with the measured current is excellent, the two lines overlapping almost perfectly. The small ripples on the measured current (see Figure A1-5), due to the pulse forming network, are not reproduced by the calculation. In addition, the pulses following the initial one, which are due to the load not being matched to the delay line, are not reproduced; relative little power is in these pulses.

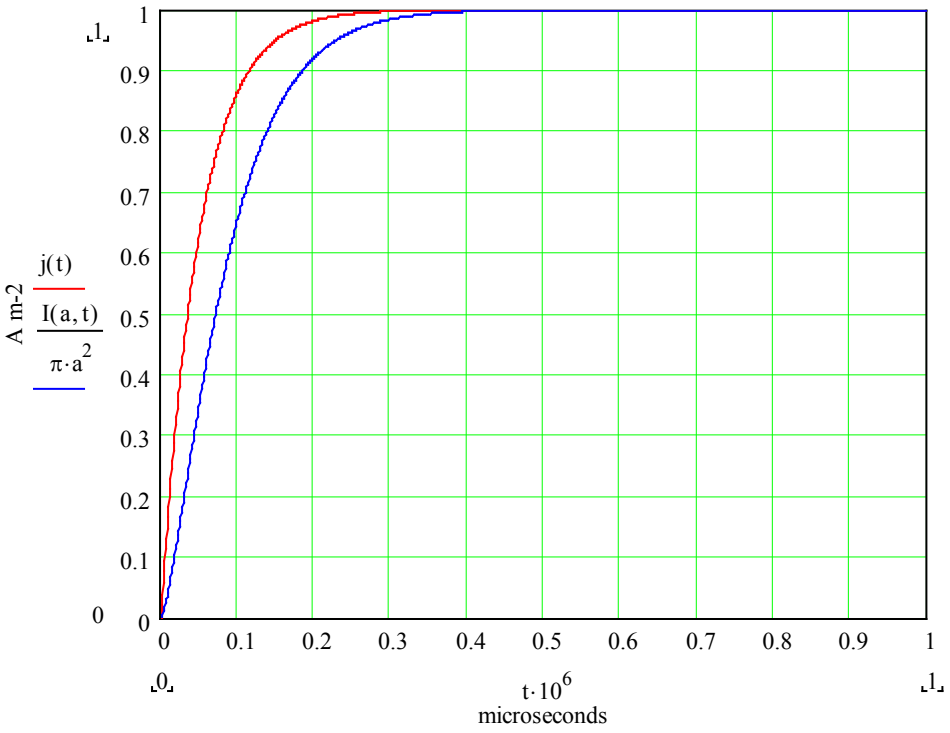

Figure A1-4. The current density (red curve) and the current (blue curve) as a function of time from (A1-17) and integrated over the radius of the wire. The current is divided by the cross sectional area to normalise the current for comparison to the current density. Tantalum wire.

[4] The Mathematics of Diffusion, J. Crank, Oxford University Press, 1967.

Figure A1-5 shows the measured current profile (green dots) overlaid on Figure A1-4 and roughly fitted to the blue curve - the calculated current profile. The agreement is good.

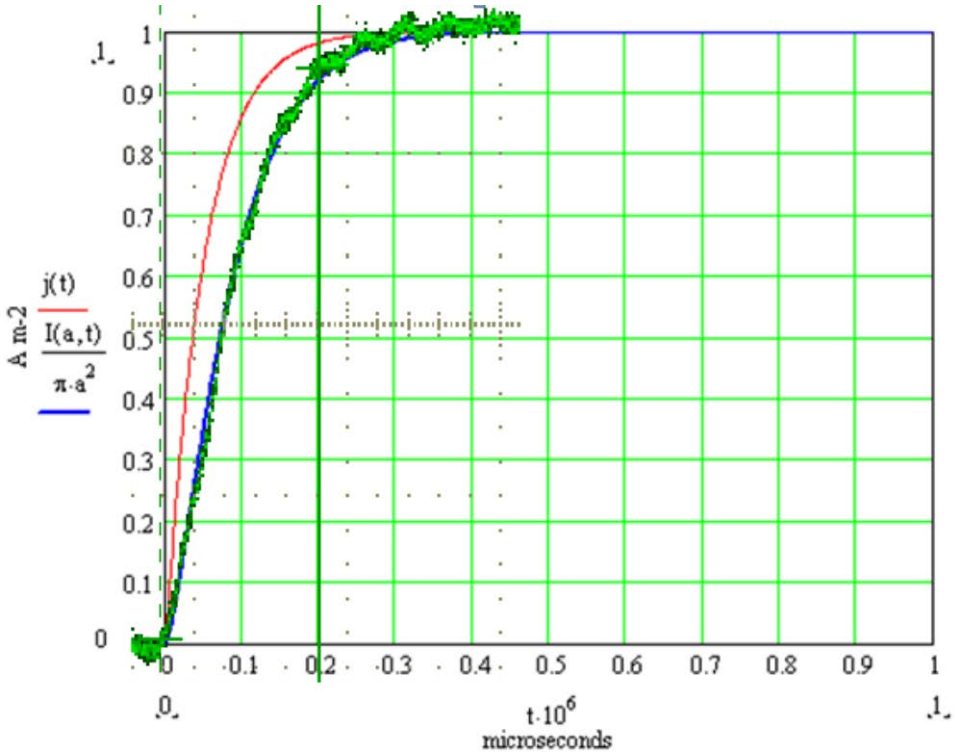

Figure A1-5. The calculated current from Figure A1-4 (the blue line) overlaid by the measured current (green dots).

The current density as a function of radius and time from A1(16), is shown in Figure A1-6. The current density is over 90% at all radii by 300 ns.

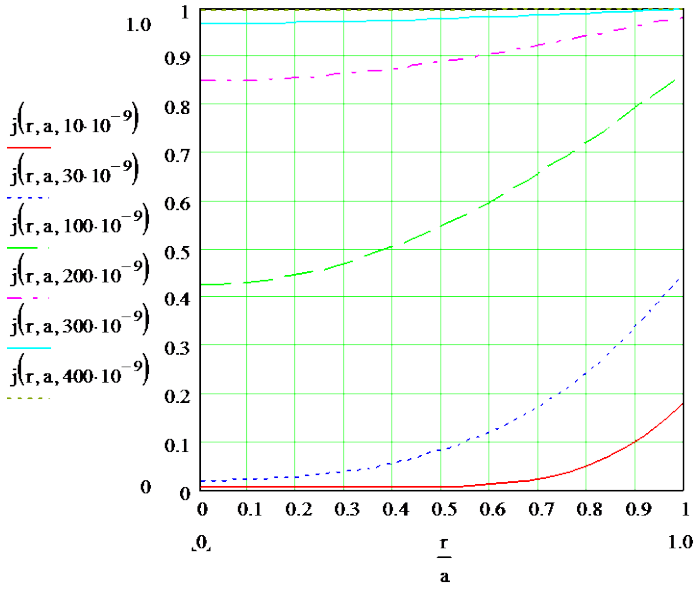

Figure A1-6. Current density as a function of radius, r/a, at different times, $1/\gamma$ = 50 ns and a = 0.25 mm.

The power density is $j^2\rho$; ignoring the resistivity, Figure A1-7 shows j^2 as a function of r/a. The power density is over 90% at all radii by 300 ns.

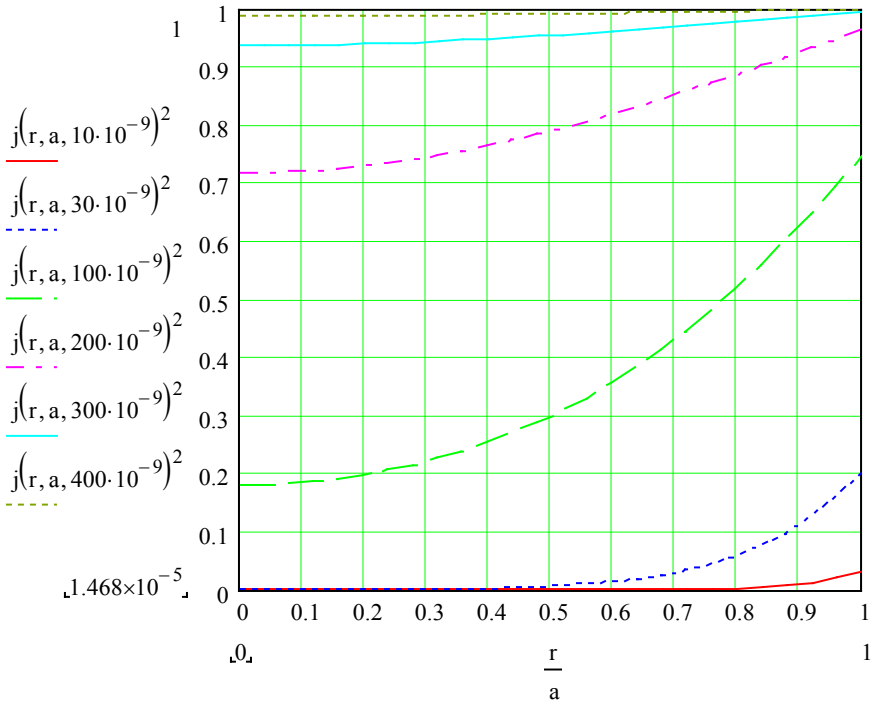

Figure A1-7. Power density (j^2) as a function of r/a at different times; a = 0.25 mm.

The energy received by the wire during the pulse determines the peak temperature rise. The power density is integrated over a period of time from 0 to 1 μs (the approximate pulse length) at different radii in the wire. The value of the power density at the outer radius of the wire, $r = a$, is used to normalise the results. Hence the values plotted are,

$$q(r,t) = \frac{\int_0^t j(r,t)^2\,dt}{\int_0^t j(a,t)^2\,dt} \qquad \text{(A1-18)}$$

against t for different values of r, as shown in Figure A1-8.

At the end of the pulse ~1 μs the centre of the wire has received 90% of the maximum energy density that is delivered to the wire at the outer radius of the wire, $r = a$. Hence, the maximum variation in energy density with radius is only 10%. So the wire receives almost uniform energy density and hence temperature rise and radial thermal stress across the radius. Clearly a smaller diameter wire would perform even better, but wires thinner than ~ 0.5 mm diameter were found to be too weak to overcome the frictional forces of the graphite jaws in the test set up.

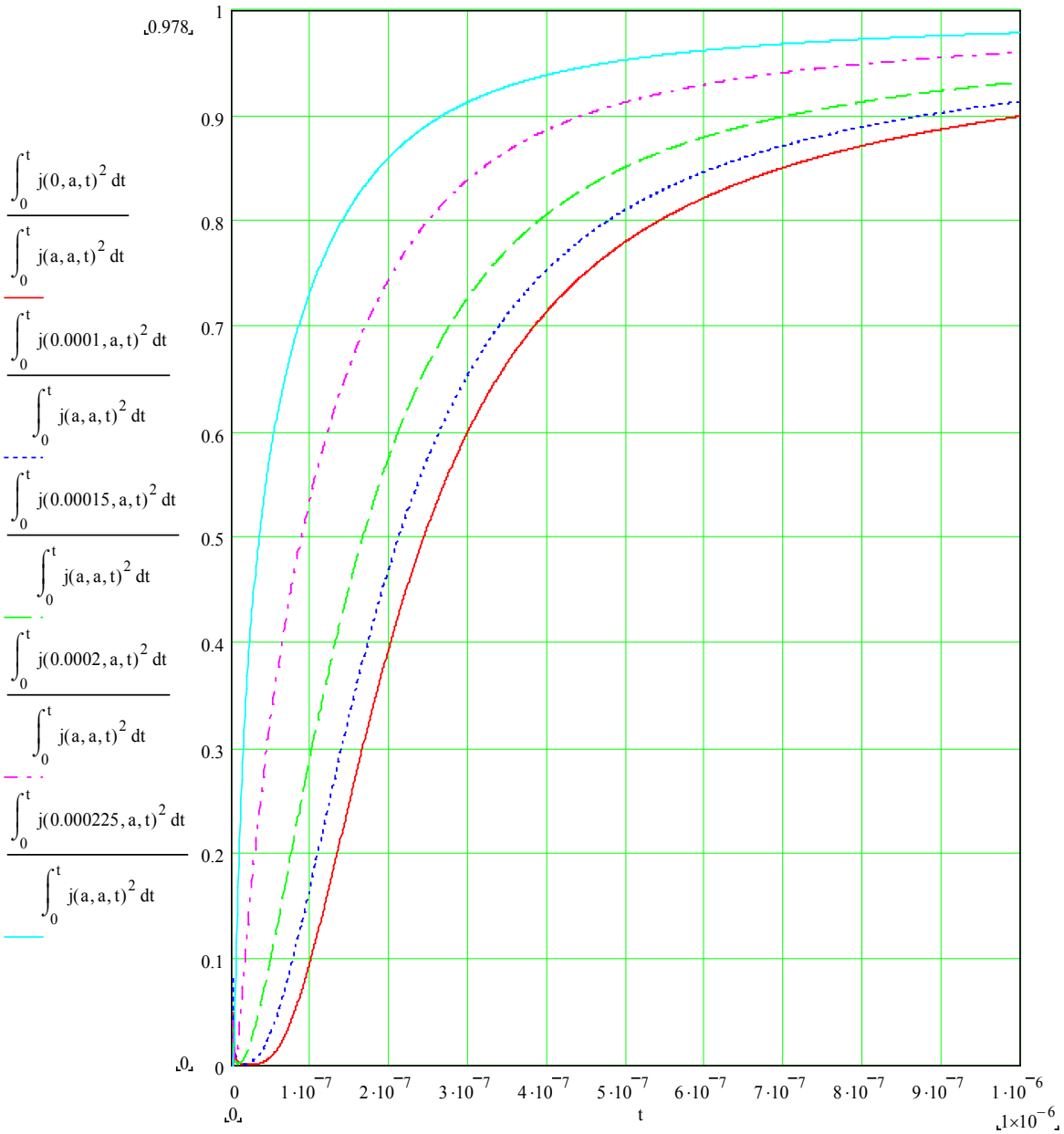

Figure A1-8. Energy density as a fraction of the energy density at radius *a*, and as a function of integrated time at radii *r* = 0, 0.1, 0.15, 0.2 and 0.225 mm.

Appendix 2. The Coefficient of Linear Thermal Expansion - a Note of Explanation

Reference [10] gives the equation fitting the thermal expansion in terms of the fractional increase in length $\Delta L/L$ (or thermal strain, ε_{th}) as a function of temperature as,

$$\frac{\Delta L}{L} = \varepsilon_{th}(T) = \left(5.8356 \cdot 10^{-7} T^2 + 3.9108 \cdot 10^{-3} T - 8.6188 x 10^{-3}\right) 10^{-3} \qquad \text{A2(1)}$$

Therefore the length varies as,

$$L(T) = L + \Delta L(T) = L\left[1 + \varepsilon_{th}(T)\right] \qquad \text{A2(2)}$$

where L is the length at the initial or reference temperature of 20°C and ΔT is the temperature rise (°C). It is interesting to note that the thermal strain is small and positive at 20°C where the majority of the measurements started from. One would have expected ε_{th} to be zero at the starting point since the temperature rise is zero.

Reference [10] also calculates the instantaneous and mean coefficients of thermal expansion, with no clear definition of these coefficients. The instantaneous coefficient, α_i, gives the value at any one temperature. The integral of this over the total range of the temperature rise gives the mean value, α_m. The mean coefficient times the total temperature rise equals the increase in length, so,

$$L(T) = L\left[1 + \alpha_m(T)\Delta T\right] \qquad \text{A2(3)}$$

Hence the value of α given in Section 7 is the mean coefficient of thermal expansion, α_m, or $\alpha\Delta T$ is equal to $\varepsilon_{th}(T)$.